XV Congresso Brasileiro de Engenharia Mecânica
15th Brazilian Congress of Mechanical Engineering
22 - 26 de Novembro de 1999 / November 22 - 26, 1999 Águas de Lindóia, São Paulo,

A FRAMEWORK TO CORRELATE EFFECTS OF CONSTRAINT LOSS AND DUCTILE TEARING ON FRACTURE TOUGHNESS – PART III : PARAMETER CALIBRATION AND FRACTURE TESTING

Claudio Ruggieri
Department of Naval Architecture and Ocean Engineering, University of São Paulo
São Paulo, SP 05508–900, E-mail: cruggi@usp.br, Brazil

Abstract *– This paper presents a newly developed procedure to calibrate the Weibull stress parameters (m, σ_u) which builds upon a scaling methodology to correct measured toughness distributions for different crack configurations. Detailed numerical analyses employing a modified boundary layer (MBL) model and 3-D finite element analyses for a standard 1(T) SE(B) specimen show the strong effect of constraint loss on individual fracture toughness values for different material properties. Such results provide compelling support to construct the parameter calibration scheme proposed in this study. The calibration procedure is then applied to determine the Weibull stress parameter, m (the Weibull modulus) for a structural C-Mn steel (BS 4360 Grade 50D).*

Key words: *cleavage fracture, statistical effects, weakest link, local approach, Weibull stress*

1. INTRODUCTION

Parts I and II of this article [1,2] described a methodology, based upon a local failure model employing the statistics of microcracks (weakest link philosophy), to predict the strongly interacting effects of constraint variations and ductile tearing on (macroscopic) cleavage fracture toughness (J_c). In particular, a probabilistic fracture parameter – the Beremin's Weibull stress (σ_w) [3]– was introduced to provide a robust coupling between the microregime of fracture and macroscopic crack driving forces (such as the J-integral). Applications of this methodology in fracture assessments relies on the notion of the Weibull stress as a crack-tip driving force [4-7]. The central feature in the predictive framework is the simple axiom that unstable crack propagation (cleavage) occurs at a critical value of the Weibull stress; under increased remote loading (as measured by J), differences in evolution of the Weibull stress reflects the potentially strong variations of near-tip stress fields. In this context, the Weibull modulus, m, plays a major role in the process to correlate effects of constraint loss and ductile tearing for varying crack configurations. Consequently, robust schemes to calibrate the Weibull parameters (m, σ_u) become a key element in fracture assessment procedures based upon σ_w.

A number of studies has demonstrated the potential capability of Weibull stress based approaches to predict constraint and ductile tearing effects on measured distributions of J_c-values and CTOD-values for structural steels [4,10,15]. The *apparent* success of these research efforts has prevented, until recently, a more active pursuit of improved schemes to calibrate parameters (m, σ_u). In spite of the promise evident in those works, difficulties still persist in the calibration of Weibull stress parameters under specific testing conditions as details of the analysis procedures (e.g. finite strain plasticity, 2-D vs 3-D, etc.) and the mesh refinement adopted to compute the stress fields become a key factor in the calibration process using fracture specimens. Large m-values accentuate the small differences in computed stresses ahead of a blunting crack tip which strongly affect the calibrated value.

Previously developed procedures to calibrate parameters (m, σ_u) (see [3, 4-6, 10] for additional details) employ measured toughness data for cleavage fracture (such as J_c-values) to define corresponding values of the Weibull stress at fracture, denoted $\sigma_{w,c}$; these values form the basis upon which the Weibull parameters for the material are estimated without making recourse to detailed micromeasurements. Such a widely adopted methodology builds upon an iterative procedure incorporating a finite element description of the crack-tip stress fields and measured values of fracture toughness. However, as convincingly demonstrated by Gao et al. [11] and Ruggieri et al [12], a major point of criticism of this calibration process is that a non-uniqueness arises in the calibrated values, i.e., many pairs of (m,σ_u) provide equally good correlation of critical Weibull stress values with the measured distribution of toughness data. Moreover, these works clearly show that it is not possible to calibrate a unique (m,σ_u) pair using only a single data set of toughness values.

This paper presents a newly developed procedure to calibrate the Weibull stress parameters (m, σ_u) which builds upon a scaling methodology to correct measured toughness distributions for different crack configurations. Detailed numerical analyses employing a modified boundary layer (MBL) model and 3-D finite element analyses for a standard 1(T) SE(B) specimen show the strong effect of constraint loss on individual fracture toughness values. The procedure quantifies the extent of large scale yielding (LSY) that develops in the fracture specimen as the initially strong small scale yielding (SSY) conditions diminish as deformation progresses. Such results provide compelling support to construct the parameter calibration scheme proposed in this study. The calibration procedure is then applied to determine the Weibull stress parameter, m (the Weibull modulus) for a structural C-Mn steel (BS 4360 Grade 50D).

2. COMPUTATIONAL PROCEDURES AND FINITE ELEMENT MODELS

2.1. Finite Element Procedures

The three-dimensional computations reported here are generated using the research code WARP3D [13] which: (1) implements a Mises constitutive models in a finite-strain framework, (2) solves the equilibrium equations at each iteration using a linear pre-conditioned conjugate gradient (LPCG) method implemented within an element-by-element (EBE) software architecture, (3) evaluates the J-integral using a convenient domain integral procedure and (4) analyzes fracture models constructed with three-dimensional, 8-node tri-linear hexahedral elements.

The finite element computations employ a domain integral procedure [14] for numerical evaluation of the J-Integral. A thickness average value for J is computed over domains defined outside material having the highly non-proportional histories of the near-tip fields and thus retains a strong domain (path) independence. Such J-values agree with estimation schemes based upon *eta*-factors for deformation plasticity [16]. They provide a convenient parameter to characterize the average intensity of far field loading on the crack front.

2.2. Constitutive Models

The elastic-plastic material employed in the analyses follows a J_2 flow theory with conventional Mises plasticity. The uniaxial true stress-logarithmic strain curve obeys a simple power-hardening model,

$$\frac{\epsilon}{\epsilon_0} = \frac{\bar{\sigma}}{\sigma_0} \quad \epsilon \leq \epsilon_0 \ ; \qquad \frac{\epsilon}{\epsilon_0} = \left(\frac{\bar{\sigma}}{\sigma_0}\right)^n \quad \epsilon > \epsilon_0 \tag{1}$$

where σ_0 and ϵ_0 are the reference (yield) stress and strain, and n is the strain hardening exponent.

Section 3 describes numerical solutions for the SSY boundary-layer model with $T = 0$ and a standard 1(T) SE(B) specimen with $a/W = 0.5$. These finite element analyses consider material flow properties covering most structural and pressure vessel steels: $n = 5$ ($E/\sigma_0 = 800$), 10 ($E/\sigma_0 = 500$) and 20 ($E/\sigma_0 = 300$) with $E = 206$ GPa and $\nu = 0.3$; these ranges of properties also reflect the upward trend in yield stress with the decrease in strain hardening exponent characteristic of ferritic steels. For the SE(B) specimens used in the fracture testing described in Section 4, the numerical solutions utilize a piecewise linear approximation to the measured tensile response for the material at the test temperature, $T = -120$°C given in [15].

2.3. Finite Element Models of SE(B) Specimens and SSY Model

3-D finite element analyses are described for a plane-side deep notch ($a/W = 0.5$) SE(B) specimen with $B = 25$mm [1(T)] and conventional geometry ($W/B = 2$). Here, a denotes the crack length and W is the specimen width. Fracture toughness tests at different lower shelf temperatures for a structural steel (BS 4360 Grade 50D) [15] were performed on the 3-point SE(B) specimens with size 0.5(T) and 2(T). Figure 1(a) shows the geometry and specimen dimensions of the SE(B) specimens employed in the analyses.

Figure 1(b) shows a typical finite element model constructed for analyses of the 1(T) SE(B) specimen. All other crack models have very similar features. A conventional mesh configuration having a focused ring of elements surrounding the crack front is used with a small key-hole at the crack tip; the radius of the key-hole, ϱ_0, is 10μm (0.01mm). Symmetry conditions enable analyses using one-quarter of the 3-D models with appropriate constraints imposed on the symmetry planes. The mesh has 14 variable thickness layers defined over the half-thickness ($B/2$); the thickest layer is defined at $Z = 0$ with thinner layers defined near the free surface ($Z = B/2$) to accommodate strong Z variations in the stress distribution. The quarter-symmetric, 3-D models for the SE(B) specimens typically have 18500 nodes and 16000 elements. These finite element models are loaded by displacement increments imposed on the centerplane nodes for the outermost 2 layers of elements (i.e., the two outermost row of nodes on the crack ligament plane - loading point region in Fig. 1(b)). A typical solution to load the specimen to $J = 100$ kJ/m^2 uses 100 load increments and requires ~ 10 CPU hours on a CRAY J-90 supercomputer.

Numerical solutions for stationary cracks under well-defined SSY conditions (with the T-stress term set to zero, i.e., $T = 0$) are generated by imposing displacements of the elastic, Mode I singular field on the outer circular boundary with radius R which encloses the crack ($r = R$). Such analyses follow the modified boundary layer (MBL) model [17] already described in Part II of this study [2].

Evaluation of the Weibull stress requires integration over the process zone, including the region as $r \rightarrow 0$. The SSY and all other crack models previously described have a small initial root radius at the crack front (blunt tip) which provides two numerical benefits: (1) it accelerates convergence of the finite-strain plasticity algorithms during the initial stage of blunting, and (2) it minimizes numerical problems during computation of the Weibull stress over material incident on the crack tip. To maintain consistency with the finite element models for the SE(B) specimens used to construct the $J_{LSY} \rightarrow J_{SSY}$ corrections, the SSY model has the same mesh configuration at the crack tip as the SE(B) models. The SSY model has one thickness layer of 2065 8-node, 3-D elements with plane-strain constraints imposed on all nodes.

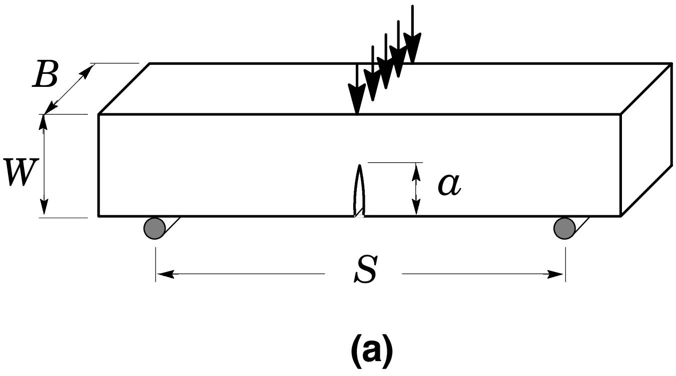

Specimen	B	W	a	a/W	S
SE(B) 0.5T	12.5	25	12.5	0.5	100
SE(B) 1T	25	50	25	0.5	200
SE(B) 2T	50	100	50	0.5	400

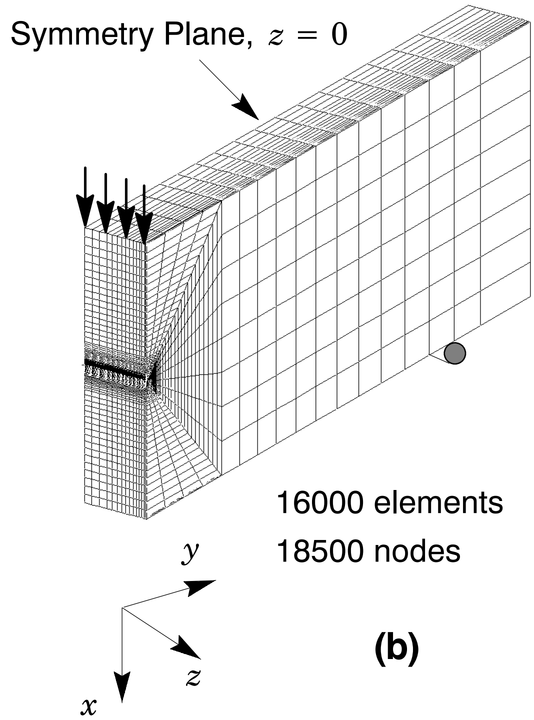

Fig. 1. SE(B) specimens with a/W = 0.5 employed in the analyses (all units in mm).

3. CALIBRATION OF WEIBULL STRESS PARAMETERS

3.1 Weibull Stress Based Constraint Corrections

This section describes the results of detailed numerical analyses employing the MBL model and 3D finite element analyses for the standard SE(B) specimens with size 1(T) to assess effects of constraint loss on individual fracture toughness values for different material properties and specimen configurations. The objective is to demonstrate the strong effect of parameter m (Weibull modulus) on $J_{LSY} \rightarrow J_{SSY}$ corrections. These results serve to introduce the framework to construct the parameter calibration scheme presented in the next section.

Figure 2 illustrates the procedure to assess the effects of constraint loss on fracture toughness needed to construct J_{LSY} *vs.* J_{SSY} trajectories. Very detailed, nonlinear 3-D finite element analyses provide the functional relationship between the Weibull stress (σ_w) and the applied loading (J) for a specified value of the Weibull modulus, m. The research code *WSTRESS* [6] is employed to compute the Weibull stress for all analyses. Based upon the argument of the Weibull stress as the crack driving force, the scaling model requires the attainment of equal values for σ_w to trigger cleavage fracture across different specimen geometries, here denoted $\sigma_{w,c}$, even though J-values may vary widely due to constraint loss. Figure 2 shows curves of σ_w *vs.* J for a standard fracture specimen (the present work employs only 1(T) deep notch SE(B) specimens) and for a plane-strain, SSY reference solution ($T/\sigma_0 = 0$) with the *same thickness of the fracture specimen*. Such curves are constructed for a fixed, representative value of the Weibull modulus, m, for each set of mechanical properties flow properties (the normalizing volume for the Weibull stress, V_0, is conveniently assigned the value of 1 mm^3). J_{LSY} values computed from the domain integral procedures in the finite element analyses of the SE(B) specimens represent thickness average values, which are consistent with experimental (average) values defined using a plastic *eta*-factor and the measured areas under the load-load line displacement curve [16]. For the plane-strain SSY model, J_{SSY} becomes simply the J value at the crack tip. Given the J_{LSY} value for the fracture specimen, the lines shown on Fig. 2 readily illustrate the technique used to determine J_{SSY}.

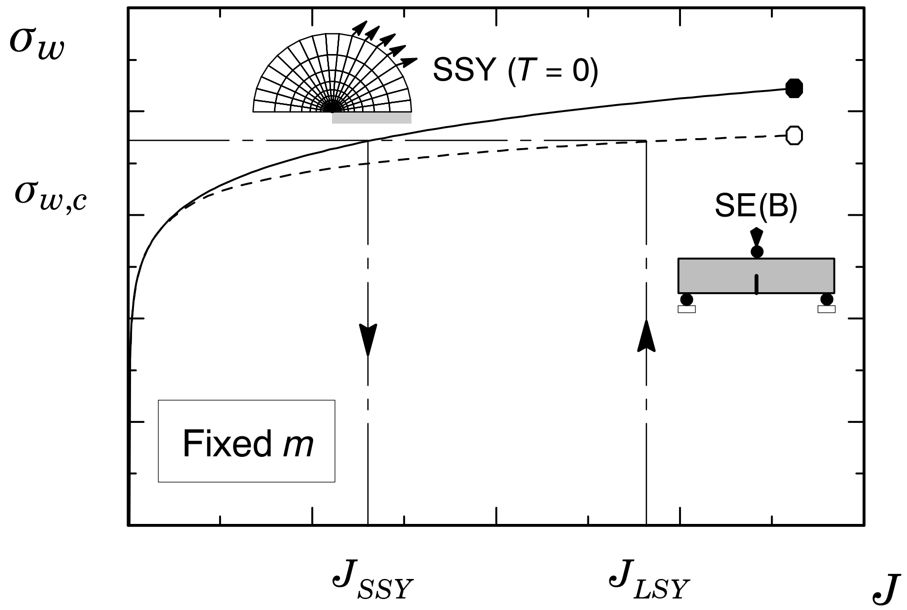

Fig. 2. Toughness scaling model used to construct $J_{LSY} \rightarrow J_{SSY}$ corrections.

Figure 5(a-d) provides the constraint corrections (LSY → SSY) for the 1(T) SE(B) specimens with different material properties ($n = 5$ with $E/\sigma_0 = 800$; $n = 10$ with $E/\sigma_0 = 500$; $n = 20$ with $E/\sigma_0 = 300$) and for varying Weibull moduli, m. The present computations consider values of $m = 10, 15, 20, 25$ and 30 to assess the sensitivity of constraint corrections on the specified Weibull modulus. These m-values are consistent with previously reported values for structural steels. Each curve provides pairs of J-values, J_{LSY} in the SE(B) specimen and J_{SSY} in SSY, that produce the same σ_w. Reference lines are shown which define a constant ratio of "constraint loss", e.g., $J_{avg} = 1.2 \times J_0$ which implies that the SE(B) average J must be 20% larger than the SSY value to generate the same Weibull stress. For each value of the Weibull modulus, the SE(B) and SSY curves agree very well early in the loading history while the SE(B) specimen maintains near SSY conditions across the crack front (recall that computation of σ_w in the SE(B) specimens considers the entire crack front). Once near-front stresses deviate from the (plane-strain) SSY levels, the σ_w curves for the SE(B) specimens fail to increase at the same rate with further loading. These results clearly illustrate the gradual nature of constraint loss in the deep-notch SE(B) specimens, especially for moderate to low hardening materials. The Weibull modulus does have an appreciable effect on predictions of constraint loss; increasing m values indicate a higher load level at the onset of constraint loss and a reduced rate of constraint loss under further loading. The larger m values, in effect, assign a greater weight factor to stresses at locations very near the crack front. The bending field, which impinges on the crack front, affects the smaller m curves more readily.

3.2 Parameter Calibration Using $\mathbf{J_{LSY}} \rightarrow \mathbf{J_{SSY}}$ Trajectories

The previous results exhibit the essential features of Weibull stress based constraint corrections for a key specimen geometry. Each SSY toughness value *corrected* from its corresponding LSY value reflects both the effects of stressed near-tip volume and the strong changes in the character of the near-tip stress fields due to constraint loss. Further, in the context of probabilistic fracture mechanics, each pair (J_{SSY}, J_{LSY}) on a given m-curve defines equal failure probabilities for cleavage fracture. Motivated by these observations, the alternative parameter calibration scheme uses the scaling methodology previously outlined to correct measured toughness distributions for different crack configurations. The procedure extends previous work by GRD [11] to calibrate parameter (m, σ_u) using high constraint (LSY) and low constraint (SSY) fracture toughness data measured at the same temperature and loading rate. Because each measured J_{LSY}-value is *corrected* to its equivalent J_{SSY}-value, the statistical (Weibull) distribution of J_{LSY}-values is also *corrected* to an equivalent statistical (Weibull) distribution of J_{SSY}-values.

Development of the calibration procedure begins by considering a statistical distribution for the toughness data. Using weakest link statistics, the well known two-parameter Weibull function conveniently characterizes the distribution of toughness values in the form (see, e.g., [18])

$$F(J_c) = 1 - \exp\left[-\left(\frac{J_c}{J_0}\right)^{\alpha}\right]. \tag{2}$$

Here, α is the Weibull modulus (*shape* parameter) for the J_c-distribution and J_0 is the characteristic toughness (*scale* parameter). This limiting distribution remains applicable for other measures of fracture toughness, such as K_{Ic} or CTOD. Previous work has also demonstrated that, under SSY conditions, the scatter in cleavage fracture toughness data is characterized by $\alpha = 2$ for J_c-distributions [10] or $\alpha = 4$ for K_{Ic}-distributions [8].

Consequently, our scheme defines the calibrated value of m for the material as the value that *corrects* the characteristic toughness J_0^{LSY} (i.e., the scale parameter of Eq. (2)) to its equivalent J_0^{SSY}. Because parameter m is assumed independent of specimen geometry (as long as the framework upon which the Weibull stress is based remains valid), the scheme remains equally applicable when two sets of fracture toughness data from different crack configurations, but with sufficient differences in the evolution of σ_w vs. J, are used (e.g., 1(T) SE(B) specimens with $a/W = 0.5$ and $a/W = 0.15$).

The following steps describe a summary of key procedures in the proposed calibration [11,12]. Section 4 illustrates the process for a ferritic structural steel (BS 4360 Gr 50 D).

Step 1

Test two sets of specimens with different crack configurations (**A** and **B**) in the DBT region to generate two distributions of fracture toughness data. Select the specimen geometries and the common test temperature to insure different evolutions of constraint levels for the two configurations. No ductile tearing should develop prior to cleavage fracture in either sets of tests.

Step 2

Perform detailed, 3-D finite element analyses for the tested specimen geometries. The mesh refinements must be sufficient to insure converged σ_w *vs.* J histories for the expected range of m-values and loading levels.

Step 3

3.1 Assume an m-value. Compute the σ_w *vs.* J history for configurations **A** and **B** to construct the toughness scaling model relative to both configuration.

3.2 Constraint correct $J_0^{\mathbf{B}}$ to its equivalent $J_{0,m}^{\mathbf{A}}$ (i.e., the corrected value of the scale parameter for the assumed m-value). Define the error of toughness scaling as $R(m) = (J_{0,m}^{\mathbf{A}} - J_0^{\mathbf{A}})/J_0^{\mathbf{A}}$. If $R(m) \neq 0$, repeat *3.1–3.2* for additional m-values.

3.3 Plot $R(m)$ *vs.* m. The calibrated Weibull modulus makes $R(m) = 0$ within a small tolerance.

Step 4

Compute the σ_u-value. After m is determined, σ_u is obtained easily from the σ_w *vs.* J history for the calibrated m-value. σ_u equals the Weibull stress value at $J = J_0^{\mathbf{A}}$ or $J = J_0^{\mathbf{B}}$ in the corresponding configuration.

4. CALIBRATION OF WEIBULL MODULUS FOR A STRUCTURAL STEEL

4.1 Fracture Toughness Testing Using SE(B) Specimens

Wiesner and Goldthorpe [15] provide cleavage fracture toughness values at different lower shelf temperatures obtained from testing of 3-point SE(B) specimens (plane-sided) with fixed crack length to width ratio, $a/W = 0.5$, and varying specimen tickness, B. The specimens have $B = 12.5$mm, 25mm and 50mm with width $W = 2B$ and span $S = 8B$ (refer to Fig. 1). The material is a ferritic C-Mn steel (BS 4360 Grade 50D) with high strain hardening ($\sigma_u/\sigma_{ys} = 1.53$). Mechanical tensile test data for this material is presented in ref. [15].

Figures 3 provides a Weibull diagram of the measured toughness values for the test temperature $T = -120$°C. The open symbols in the plots indicate the experimental fracture toughness data for the SE(B) specimens. Values of cumulative probability, F, are obtained by ordering the J_c-values and using $F = (i - 0.5)/N$, where i denotes the rank number and N defines the total number of experimental toughness values. The straight lines indicate the two-parameter Weibull distribution obtained by a maximum likelihood analysis of the data set. The maximum likelihood estimates $(\hat{\alpha}, \hat{J}_0)$ for each data set are: (1.5, 44.3) for the 0.5(T) specimen; (2.6, 51.6) for the 1(T) specimen and (1.4, 29.3) for the 2(T) specimen. Note that the α-values of the Weibull distribution for J_c deviate significantly from $\alpha = 2$.

4.2 Parameter Calibration

The procedure used here to calibrate the Weibull stress parameters for the C-Mn steel follows the proposed scheme outlined in Section 3.2. In the present application, we calibrate parameter m by *scaling* the measured toughness distribution for the 0.5(T) SE(B) specimen to an equivalent toughness distribution for the 2(T) SE(B) specimen. Very detailed finite element computations of these specimens enables construction of the $J_{0.5(\mathrm{T})} \rightarrow J_{2(\mathrm{T})}$ correction shown in Fig. 4. The calibration process simply becomes one of determining an m-value that corrects $J_0^{0.5(\mathrm{T})}$ to its equivalent $J_0^{2(\mathrm{T})}$.

A central feature of this methodology also lies in the choice of parameter α describing the scatter of the toughness distribution. The procedure adopts a *fixed* value $\alpha = 2$ to describe the distribution of J_c-values which makes contact with the probabilistic treatment of fracture under SSY conditions based upon weakest link statistics [6,11,12]; however, previous analyses [12] reveal a week dependence of J_0 on α. For the SE(B) specimens with $B = 12.5$mm at $T = -120$°C, the maximum likelihood estimate of $J_0^{0.5(\mathrm{T})}$ with $\alpha = 2$ is 49.3 kJ/m^2 and differs by 11% from the previous value of 44.3 kJ/m^2 (recall the large deviations of the Weibull modulus from $\alpha = 2$ for this data set). Similarly, for the SE(B) specimens with $B = 50$mm at $T = -120$°C, the maximum likelihood estimate of $J_0^{0.5(\mathrm{T})}$ with $\alpha = 2$ is 34.0 kJ/m^2 and differs by 12% from the previous value of 29.3 kJ/m^2. With the introduction of a *fixed* value $\alpha = 2$, our calibration proce-

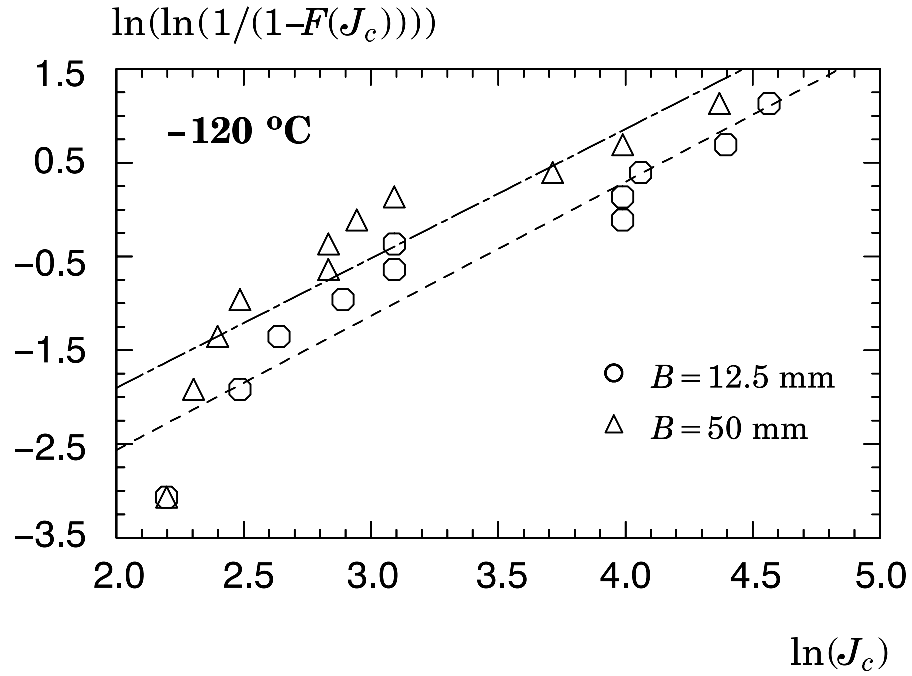

Fig. 3. Weibull plots of toughness values at T = −120°C.

dure yields $m \approx 15$ for the steel tested at $T = -120$°C. Figure 4 illustrates the graphical procedure to determine parameter m.

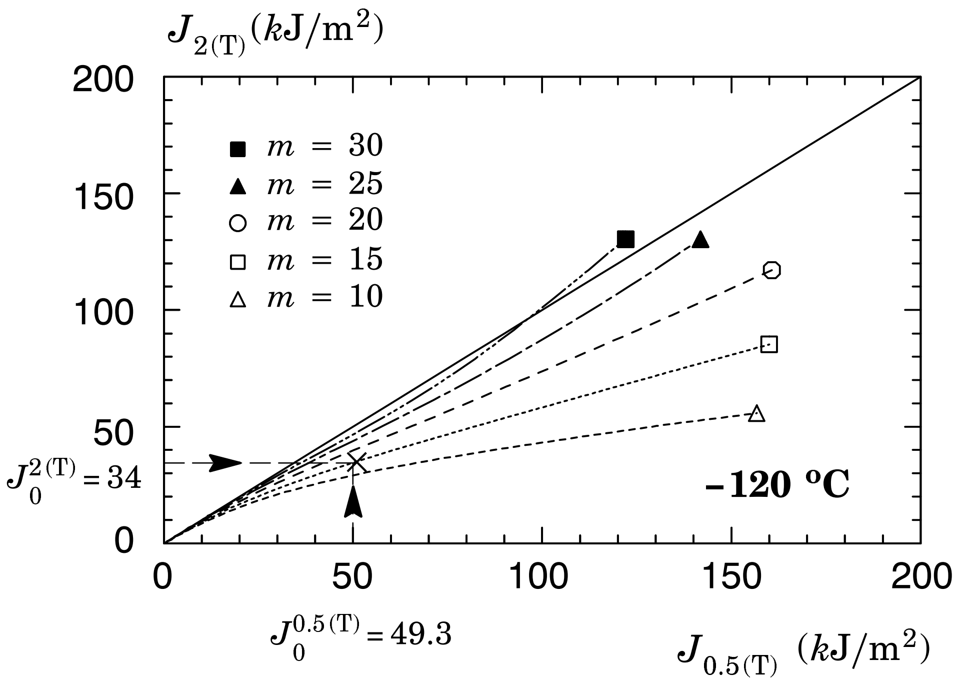

Fig. 4. $J_{0.5(T)} \rightarrow J_{2(T)}$ correction using a scaling methodology based upon the Weibull stress with varying Weibull moduli for tested structural steel BS4360 Gr50. The lines on the plot indicates the calibration process to determine parameter m.

5. CONCLUDING REMARKS

Our extensive numerical analyses to assess constraint loss effects (LSY → SSY) for standard, deep notch SE(B) specimens demonstrate the strong influence of the Weibull stress parameter m (Weibull modulus) on $J_{LSY} \rightarrow J_{SSY}$ corrections. These analyses provide support to introduce an alternative, improved procedure based upon a toughness scaling model to calibrate the Weibull stress parameters, (m, σ_u). The toughness scaling model enables construction of Weibull stress based constraint corrections for experimentally measured J_c-values to provide the Weibull parameters for a structural C-Mn steel (BS 4360 Grade 50D). Further work is in progress to validate the proposed procedure as a more general and robust scheme to calibrate the Weibull stress parameters for several crack configurations and its implication on predictions of toughness distributions and fracture assessment procedures.

Acknowledgements

This investigation was supported by grants principally from the Scientific Foundation of the State of São Paulo (FAPESP) under Grant 98/10574-2. Access to the Cray J-90 and SGI-Origin 200 at the High Performance Computing Center (LCCA) of the University of São Paulo is also acknowledged.

References

1. Ruggieri, C., "A Framework to Correlate Effects of Constraint Loss and Ductile Tearing on Fracture Toughness – Part I: Probabilistic Approach," *15th Brazilian Congress of Mechanical Engineering (Cobem 99)*, Águas de Lindóia, Brazil (1999).
2. Trovato, E. and Ruggieri, C., "A Framework to Correlate Effects of Constraint Loss and Ductile Tearing on Fracture Toughness – Part II: Fracture Under Small Scale Yielding Conditions," *15th Brazilian Congress of Mechanical Engineering (Cobem 99)*, Águas de Lindóia, Brazil (1999).
3. Beremin, F.M, "A Local Criterion for Cleavage Fracture of a Nuclear Pressure Vessel Steel," *Metallurgical Transactions,* Vol. 14A, pp. 2277–2287, 1983.
4. Ruggieri, C. and Dodds, R. H., "A Transferability Model for Brittle Fracture Including Constraint and Ductile Tearing Effects: A Probabilistic Approach," *International Journal of Fracture*, Vol. 79, pp. 309-340, 1996.
5. Ruggieri, C. and Dodds, R. H., "Probabilistic Modeling of Brittle Fracture Including 3-D Effects on Constraint Loss and Ductile Tearing," *Journal de Physique*, Vol. 1996.
6. Ruggieri, C. and Dodds, R. H., "WSTRESS Release 1.0: Numerical Computation of Probabilistic Fracture Parameters for 3-D Cracked Solids," *BT–PNV–30 (Technical Report)*, EPUSP, University of São Paulo, 1997.
7. Ruggieri, C., Dodds, R. H. and Wallin, K., "Constraints Effects on Reference Temperature, T_0, for Ferritic Steels in the Transition Region," *Engineering Fracture Mechanics*, Vol. 60, pp. 19-36, 1998.
8. Wallin, K. "The Scatter in K_{Ic} Results," *Engineering Fracture Mechanics,* Vol. 19, pp. 1085–1093, 1984.
9. Mudry, F., 1987, "A Local Approach to Cleavage Fracture", *Nuclear Engineering and Design*, Vol. 105, pp. 65–76.
10. Minami, F., Brückner–Foit, A., Munz, D.and Trolldenier, B., "Estimation Procedure for the Weibull Parameters Used in the Local Approach," *International Journal of Fracture*, Vol. 54, pp. 197–210, 1992.
11. Gao,X., Ruggieri, C. and Dodds, R. H., "Calibration of Weibull Stress Parameters Using Fracture Toughness Data". (*Submmitted for Publication*).
12. Ruggieri, C., Gao, X. and Dodds, R. H., "Transferability of Elastic-Plastic Fracture Toughness Using the Weibull Stress Approach: Significance of Parameter Calibration". (*Submmitted for Publication*).
13. Koppenhoefer, K., Gullerud, A., Ruggieri, C., Dodds, R. and Healy, B., "WARP3D: Dynamic Nonlinear Analysis of Solids Using a Preconditioned Conjugate Gradient Software Architecture", *Structural Research Series (SRS) 596*, UILU–ENG–94–2017, University of Illinois at Urbana–Champaign, 1994.
14. Moran, B., and Shih, C.F., "A General Treatment of Crack Tip Contour Integrals", *International Journal of Fracture,* Vol. 35, pp. 295–310, 1987.
15. Wiesner, C. S. and Goldthorpe, M. R., "The Effect of Temperature and Specimen Geometry on the Parameters of the Local Approach to Cleavage Fracture" in *International Conference on Local Approach to Fracture (MECAMAT 96)*, Fontainebleau, France, 1996, pp. C6-295–304.
16. Kirk, M.T. and Dodds, R.H., "*J* and *CTOD* Estimation Equations for Shallow Cracks in Single Edge Notch Bend Specimens," *Journal of Testing and Evaluation*, Vol. 24, No. 4, pp. 228–238, 1993.
17. Larsson, S. G. and Carlsson, A. J., "Influence of Non–Singular Stress Terms and Specimen Geometry on Small Scale Yielding at Crack–Tips in Elastic–Plastic Materials", *Journal of the Mechanics and Physics of Solids*, Vol. 21, pp. 447–473, 1973.
18. Mann, N. R., Schafer, R. E. and Singpurwalla, N. D., *Methods for Statistical Analysis of Reliability and Life Data*, Jonh Wiley & Sons, New York, 1974.

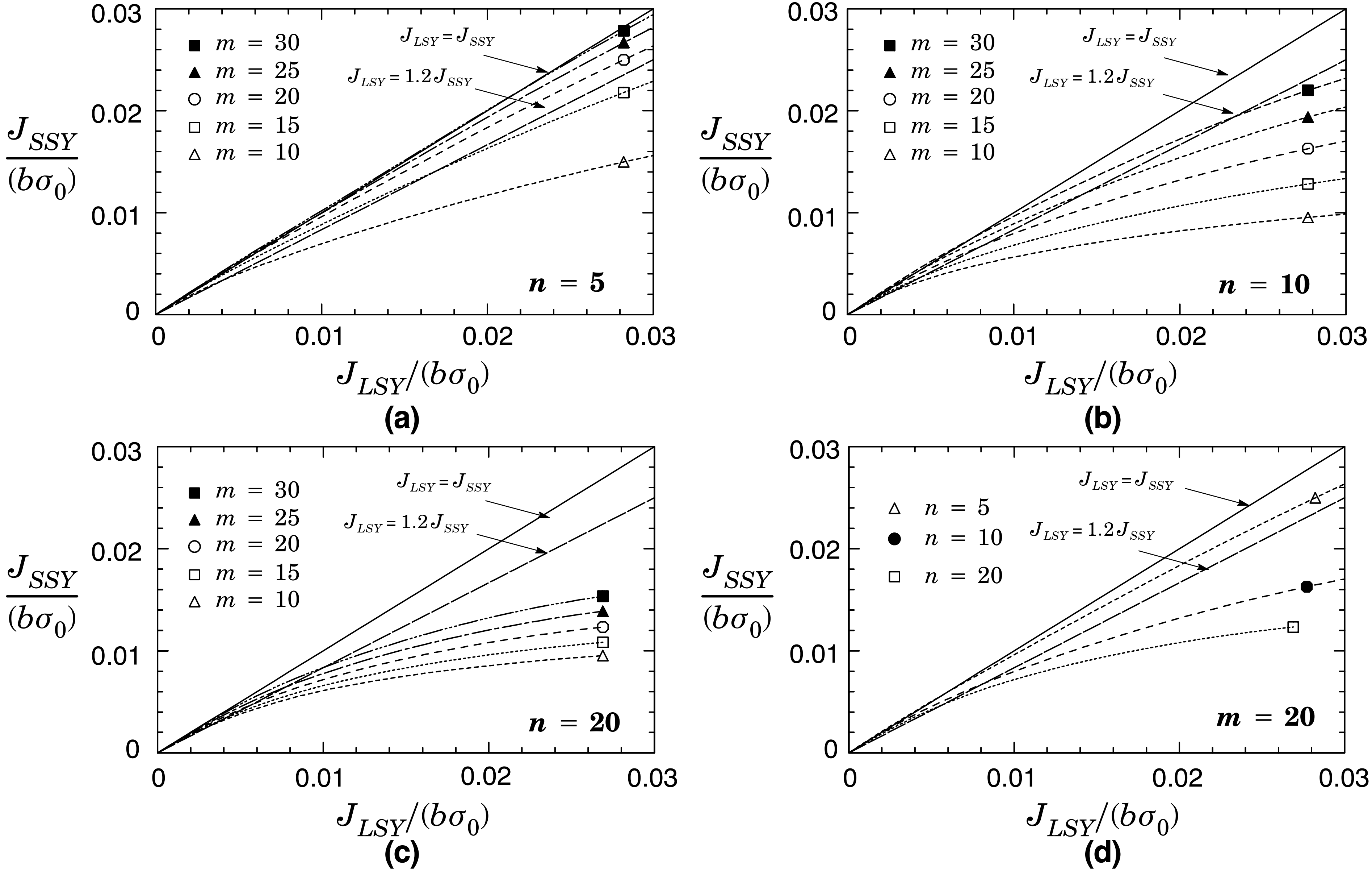

Fig. 5. $J_{LSY} \rightarrow J_{SSY}$ correction using a scaling methodology based upon the Weibull stress with varying Weibull moduli for plane-sided 1(T) SE(B) specimens.